SPECIFICATIONS AND PERFORMANCE OF A CHICANE MAGNET FOR THE cERL IR-FEL

N. Nakamura[†], K. Harada, N. Higashi, Y. Honda, R. Kato, C. Mitsuda, S. Nagahashi, T. Obina,
H. Sakai, M. Shimada, H. Takaki, O. A. Tanaka
High Energy Accelerator Research Organization (KEK), Tsukuba, Japan
Y. Lu, The Graduate University for Advanced Studies (Sokendai), Hayama, Japan

Abstract

A chicane magnet was newly installed between two undulators of the IR-FEL in the cERL in order to increase the FEL gain and pulse energy by converting the energy modulation to the density modulation in an electron bunch. It consists of three dipole magnets with laminated yokes made of 0.1-mm-thick permalloy sheets and the coil currents of the three magnets are independently controlled by three power supplies with the maximum current of 10 A. The current ratio of the three dipole magnets was tuned after installation to make its orbit bumps closed and then the chicane magnet was used in the FEL operation. We present the specifications and operational performance of the chicane magnet.

INTRODUCTION

The IR-FEL was constructed in the Compact ERL (cERL) at KEK from October 2019 to May 2020 for the purpose of developing high-power mid-infrared lasers for high-efficiency laser processing utilizing molecular vibrational photo-absorption [1]. The role of the chicane magnet is to increase the FEL gain and pulse energy by converting the energy modulation to the density modulation of an electron bunch (microbunching), shown in Fig. 1.
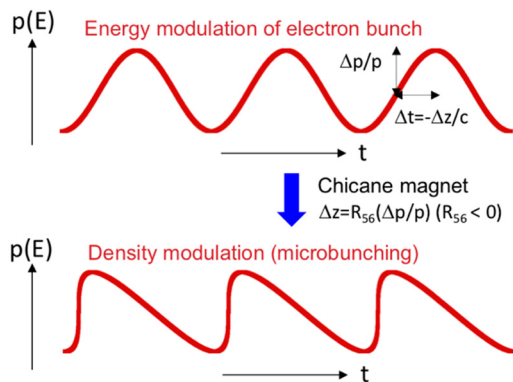
Figure 1: Schematic illustration of the effect of the chicane magnet in an FEL. R_{56} means the longitudinal dispersion of the chicane magnet.

The chicane magnet was installed between the two 3-m FEL undulators [2]. Figure 2 shows layout of the cERL FEL components including the chicane magnet between the undulators. In this paper, we describe specifications, field distribution and bump orbits, tuning of bump orbits and operational performance of the chicane magnet.

---

† noro.nakamura@kek.jp
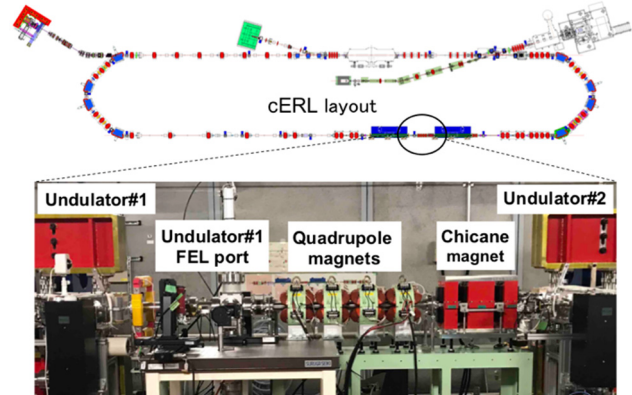
Figure 2: Layout of cERL components including the chicane magnet between the two FEL undulators.

SPECIFICATIONS

Figure 3 shows the chicane magnet installed in the cERL. The chicane magnet consists of three dipole magnets BMIS01, 02 and 03. The yoke lengths are 70, 140 and 70 mm for BMIS01, 02 and 03 respectively and the total length of the chicane magnet is 458 mm including the coils. The yoke width and height are 180 and 270 mm and the magnetic gap is 32 mm. The yokes of the chicane magnet are made of 0.1-mm thick laminated permalloy with high permeability and low hysteresis and eddy currents. The turn number of the magnet coil made of a copper wire is 168 and the coil current of each dipole magnet is independently provided by a power supply up to 10 A. The specification of the chicane magnet is showed in Table 1. The chicane magnet was originally produced as the phase shifter prototype of a polarization-controlled undulator and reused for the cERL IR-FEL [3].

Figure 3: Chicane magnet installed in the cERL.

Table 1: Specifications of the Chicane Magnet

Yoke	
Material	0.1-mm permalloy lamination
Permeability	400000 (max.)
Saturation field	0.75 T
Adhesive	Varnish
Coil	
Turn number	168
Material	Copper wire (2 × 3 mm)
Adhesive	Epoxy resin
Current/turn	10 A (max.)

FIELD DISTRIBUTION AND ORBITS

Figure 4 shows the measured and calculated longitudinal field distributions on the central axis of the chicane magnet at coil currents of $I_{BMIS01} = I_{BMIS03} = 6.96$ A and $I_{BMIS02} = 8.33$ A. The current ratio, $R \equiv I_{BMIS01}/I_{BMIS02} = I_{BMIS03}/I_{BMIS02}$, is 0.8357 and makes the bump orbit closed.
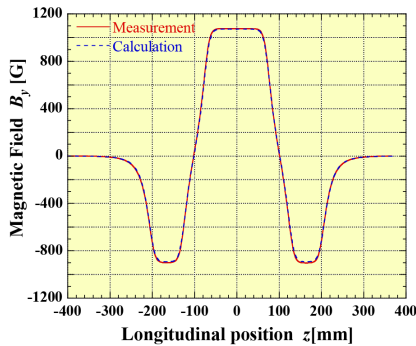
Figure 4: Measured and calculated magnetic fields of the chicane magnet along the center axis at coil currents of $I_{BMIS01} = I_{BMIS03} = 6.96$ A and $I_{BMIS02} = 8.33$ A.

Figure 5 shows closed bump orbits calculated from the field distribution on the central axis for different coil currents with the current ratio of $R = 0.8357$. The maximum closed orbit bump made by the magnetic field has the longitudinal dispersion(R_{56}) of -6 mm at $I_{BMIS02} = 10$ A. Eqs. (1) to (3) are used for these calculations.

$$x'(z) = \frac{e}{mc\gamma\beta} \int_{-\infty}^{z} B_y(z_1)dz_1 \tag{1}$$

$$x(z) = \frac{e}{mc\gamma\beta} \int_{-\infty}^{z} dz_2 \int_{-\infty}^{z_2} B_y(z_1)dz_1 \tag{2}$$

$$R_{56} = -\int_{-\infty}^{\infty} x'(z)^2 dz = -2\Delta L_z \tag{3}$$

Here c, e, m, γ, β, x, x' and ΔL_z are the velocity of light, electron charge and mass, Lorentz factor, velocity divided by the velocity of light, the horizontal position and angle

and the path-length of the electron beam. Figure 6 shows the horizontal distribution of the magnetic field at the center of BMIS02. The central axis of the chicane magnet is horizontally displaced from the beam-orbit center by 5 mm to keep a good field uniformity for a large bump height.
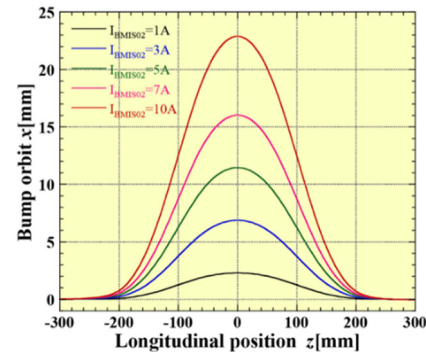
Figure 5: Calculated closed bump orbits made by the chicane magnet for $I_{BMIS02} = 1, 3, 5, 7, 10$ A with $R = 0.8357$.
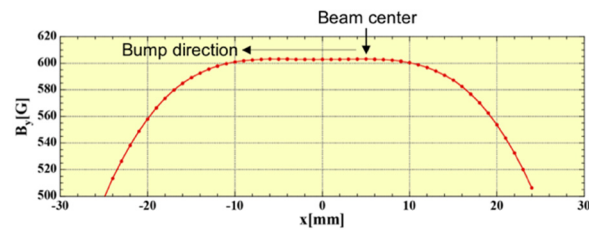
Figure 6: Horizontal distribution of the measured vertical magnetic field at the center of BMIS02 for $I_{BMIS02} = 4.67$ A.

TUNING OF BUMP ORBITS

Tuning of bump orbits was carried out in June 2020 by use of the screen monitor (cam23C) in Undulator #2 downstream of the chicane magnet in order to make the bump orbits closed. The current ratio of the three dipole magnets for the closed bump orbit was measured and the measured data was fitted to a sixth order polynomials as shown in Fig. 7. The current ratio was kept almost constant at $R = 0.834$ up to $I_{BMIS02} = 6$ A, but it significantly changed with the beam profile for more than 6A, probably because the horizontal field uniformity was degraded for the large bump heights. Figure 8 shows beam profiles at the screen monitor for $I_{BMIS02} = 0, 5, 6$ and 7 A.
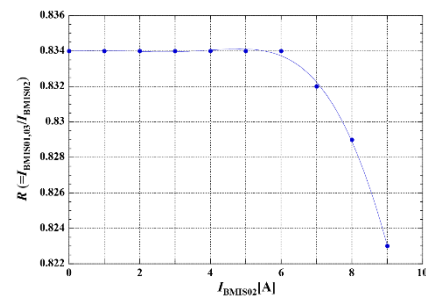
Figure 7: Current ratio of the chicane magnet as a function of I_{BMIS02} for making the bump orbit closed and the fitted sixth-order polynomial curve.

MC2: Photon Sources and Electron Accelerators

A18 Energy Recovery Linacs
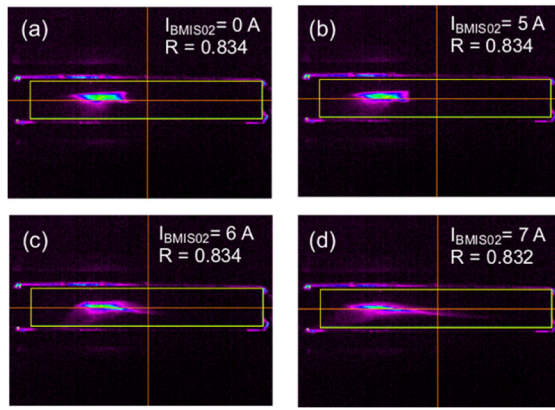
Figure 8: Beam profiles with I_{BMIS02} = (a) 0 A, (b) 5 A, (c) 6 A and (d) 7 A at the screen monitor (cam23C) in the Undulator #2 downstream of the chicane magnet.

OPERATIONAL PERFORMANCE

The FEL commissioning was performed in two periods, June to July 2020 and February to March 2021. The FEL pulse energy was not so high in the first period, but it was several tmes increased in the second period, probably because of undulator tapering [2] and/or beam quality improvement [4].

In the FEL commissioning, the chicane magnet was sometimes excited at the FEL wavelength of about 20 μm to check the operational performance. Figure 9 shows time chart and chicane-current dependence of the FEL output in 3rd July 2020. In this case, the FEL output was enhanced by 190%. On the other hand, enhancement of the FEL output was about 30% or less in March 2021, as shown in Fig. 10. In most cases, the FEL output could be more or less increased by making use of the chicane magnet. However, it is necessary to perform more systematic study and analysis of the enhancement effect including different FEL wavelengths.
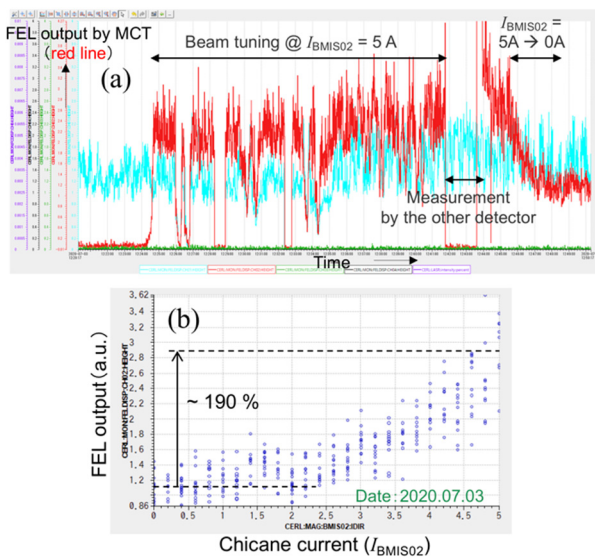
Figure 9: (a) Time chart and (b) chicane-current dependence of the FEL output measured by the MCT detector in 3rd July 2020.
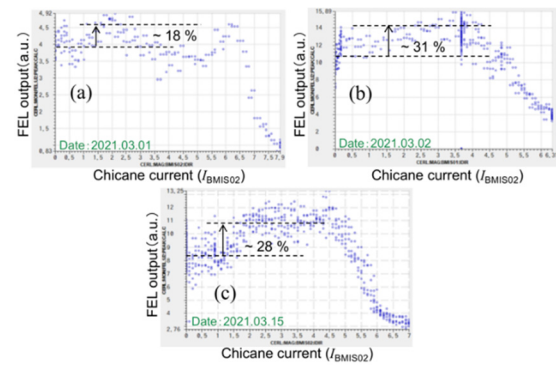
Figure 10: Chicane-current dependences of the FEL output in (a) 1st, (b) 2nd, and (c) 15th March 2021.

SUMMARY

We summarize our presentation on the chicane magnet below.

- A chicane magnet is placed between the two undulators in order to increase the FEL gain and pulse energy of the cERL IR-FEL.
- The chicane magnet consists of three dipole magnets, each of which has laminated yokes made of 0.1-mm-thick permalloy sheets and coils exciting the magnetic field with the maximum current of 10 A.
- The current ratio of the three dipole magnets for making the bump orbit closed is almost the same at I_{BMIS02} < 6 A, but it changes with the beam profile at I_{BMIS02} > 6 A, because the field uniformity on the bump orbit is degraded for large bump heights.
- The FEL output at 20 μm was enhanced in most cases by making use of the chicane magnet. The enhancement effect was different for different dates or conditions.
- More systematic study and analysis should be performed including different wavelengths to clarify the enhancement effect of the chicane magnet.

ACKNOWLEDGEMENTS

REFERENCES

[1] R. Kato *et al.*, "Construction of an Infrared FEL at the Compact ERL", presented at the *12th Int. Particle Accelerator Conf. (IPAC'21)*, Campinas, Brazil, May 2021, paper TUPAB099.

[2] M. Adachi *et al.*, to be submitted to SRI2021.

[3] N. Nakamura *et al.*, "Phase shifter prototype with laminated permalloy yokes for a polarization controlled undulator", in *Proc. of PAC09*, Vancouver, Canada, May 2009, paper MO6PFP090, pp.342-344.

[4] O. A. Tanaka, N. Higashi, and T. Miyajima, "Injector Optimization for the IR-FEL Operation at the Compact ERL at KEK", presented at the *12th Int. Particle Accelerator Conf. (IPAC'21)*, Campinas, Brazil, May 2021, paper FRXB07.